Articles

Mechanistic Studies of Palladium(II)-α-Diimine-Catalyzed Polymerizations of *cis*- and *trans*-2-Butenes

Weijun Liu and Maurice Brookhart*

Department of Chemistry, University of North Carolina at Chapel Hill, Chapel Hill, North Carolina 27599-3290

Received June 1, 2004

Complexes $[(N\wedge N)Pd(CH_3)(L)]BAr'_4$ (**3**, **4**: L = NCAr′; **5**: L = OEt_2) ($N\wedge N \equiv ArN{=}C(R){-}C(R){=}NAr$, **3**, **5**: Ar = 2,6-$C_6H_3(Me)_2$; **4**: Ar = 2,6-$C_6H_3(^iPr)_2$; Ar′ ≡ 3,5-$C_6H_3(CF_3)_2$) catalyze the polymerization of *trans*- and *cis*-2-butene. Both the productivity and the molecular weight of poly(*cis*-2-butene) are much lower than those of poly(*trans*-2-butene). The polymers exhibit atactic regioregular microstructure with a methyl group on every third backbone carbon. Low-temperature NMR studies show that migratory insertion in the η^2-butene complexes $[(N\wedge N)Pd(CH_3)(CH_3CH{=}CHCH_3)]^+$ (**6** and **11**) occurs to give isomerized alkyl olefin complexes $[(N\wedge N)Pd(CH_2CH_2CH(CH_3)_2)(CH_3CH{=}CHCH_3)]^+$ (**8** and **12**). The first insertion barrier of *trans*-2-butene (19.1 kcal/mol) is slightly lower than that of *cis*-2-butene (19.3 kcal/mol), while the subsequent insertion barrier of *cis*-2-butene (20.2 kcal/mol) is 0.6 kcal/mol higher than that for *trans*-2-butene (19.6 kcal/mol). The isopentyl palladium complexes **14a** and **14b**, which most closely model the propagating species, exhibit nearly equal binding affinities for *cis*- and *trans*-2-butene.

Introduction

A unique feature of late metal catalyst systems based on Ni(II) and Pd(II) is the ability to produce polyolefins with very different microstructures relative to those produced using early metal catalysts.[1−3] In a series of papers employing α-diimine complexes bearing bulky aryl groups as illustrated in Figure 1, we,[4−6] the DuPont group,[7,8] and subsequently others[9−12] have shown that polymerization of ethylene results in production of branched polyethylenes, while polymerization of α-olefins results in polymers with many fewer branches than expected compared to polymers produced via monomer enchainment through sequential 1,2-additions. Poly(cyclopentene) exhibits 1,3-monomer enchainment.[13]

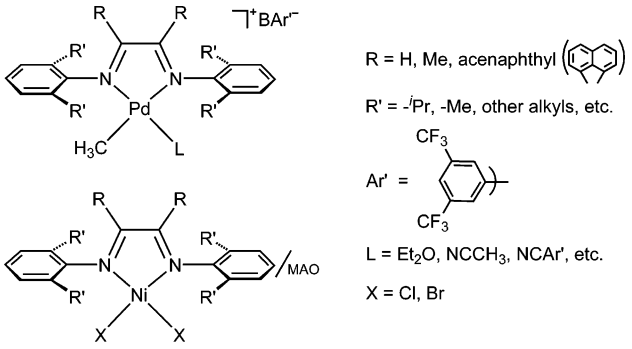

Figure 1. (α-diimine)Ni(II) and Pd(II) olefin polymerization catalysts.

These unique microstructures are attributed to the ability of Ni or Pd to migrate along the polymer chain via a series of β-hydride elimination/reinsertion reactions[14] ("chain walking") in competition with monomer insertion. For example, in the case of ethylene initial insertion forms a primary metal alkyl bond; subsequent chain walking produces secondary metal alkyl species,

(1) Ittel, S. D.; Johnson, L. K.; Brookhart, M. *Chem. Rev.* **2000**, *100*, 1169−1203.
(2) Mecking, S. *Angew. Chem., Int. Ed.* **2001**, *40*, 534−540.
(3) Gibson, V. C.; Spitzmesser, S. K. *Chem. Rev.* **2003**, *103*, 283−315.
(4) Johnson, L. K.; Killian, C. K.; Brookhart, M. *J. Am. Chem. Soc.* **1995**, *117*, 6414−6415.
(5) Killian, C. M.; Tempel, D. J.; Johnson, L. K.; Brookhart, M. *J. Am. Chem. Soc.* **1996**, *118*, 11664−11665.
(6) Gates, D. P.; Svejda, S. A.; Oñate, E.; Killian, C. M.; Johnson, L. K.; White, P. S.; Brookhart, M. *Macromolecules* **2000**, *33*, 2320−2334.
(7) Johnson, L. K.; Killian, C. M.; Arthur, S. D.; Feldman, J.; McCord, E. F.; McLain, S. J.; Kreutzer, K. A.; Bennett, A. M. A.; Coughlin, E. B.; Ittel, S. D.; Parthasarathy, A.; Tempel, D. J.; Brookhart, M. S. WO 9623010, 1996.
(8) Guan, Z.; Cotts, P. M.; McCord, E. F.; McLain, S. J. *Science* **1999**, *283*, 2059−2062.
(9) Pellecchia, C.; Zambelli, A.; Oliva, L.; Pappalardo, D. *Macromolecules* **1996**, *29*, 6990−6993.
(10) Pellecchia, C.; Zambelli, A. *Macromol. Rapid Commun.* **1996**, *17*, 333−338.
(11) Pellecchia, C.; Zambelli, A.; Mazzeo, M.; Pappalardo, D. *J. Mol. Catal. A: Chem.* **1998**, *128*, 229−237.
(12) Pappalardo, D.; Mazzeo, M.; Pellecchia, C. *Macromol. Rapid Commun.* **1997**, *18*, 1017−1023.
(13) McLain, S. J.; Feldman, J.; McCord, E. F.; Gardner, K. H.; Teasley, M. F.; Coughlin, E. B.; Sweetman, K. J.; Johnson, L. K.; Brookhart, M. *Macromolecules* **1998**, *31*, 6705−6707.
(14) Möhring, V. M.; Fink, G. *Angew. Chem., Int. Ed. Engl.* **1985**, *24*, 4, 1001−1003.

10.1021/om040077m CCC: $27.50
Publication on Web 11/20/2004

Scheme 1. Chain-Straightening Model in α-Diimine Ni(II)- and Pd(II)-Catalyzed Propylene Polymerization

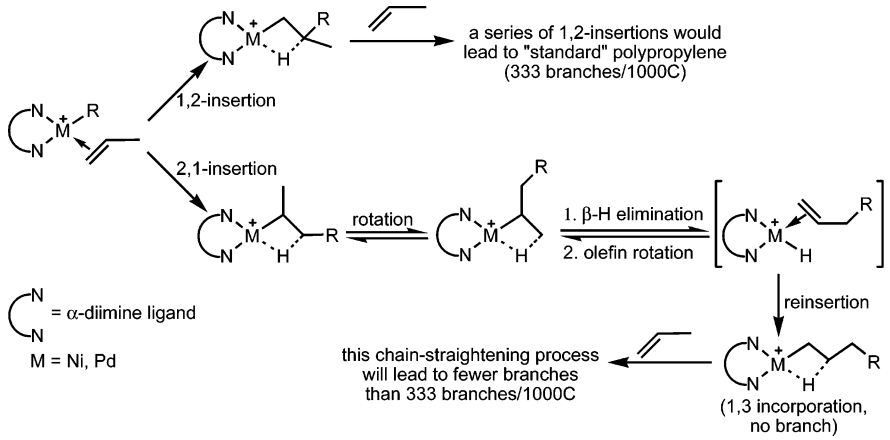

which upon migratory insertion creates a branch in the polymer chain. Fewer branches than expected in poly(α-olefin)s arise due to 2,1-insertion followed by chain walking to form a primary metal alkyl bond, which then undergoes insertion. Insertion of an α-olefin into a primary bond is sterically favored over insertion into a secondary alkyl bond. In the case of propylene, this process can result in 1,3-enchainment, as illustrated in Scheme 1.

While early metal catalysts are highly active for polymerization of α-olefins, none are known to homopolymerize disubstituted internal olefins, presumably due to steric constraints. Alternating copolymerization of ethylene and 2-butenes has been reported using early metal catalysts, as has random copolymerizations where the mole fraction of ethylene incorporated exceeds 50%.[15−19] Recently, we have reported the homopolymerization of *trans*-2-butene using Ni(II) diimine catalysts **1** and **2** (Figure 2).[20] Turnover rates at 25 °C are ca.

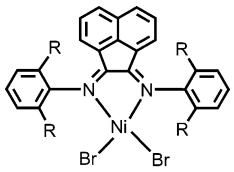

Figure 2. (α-dimine)Ni(II) complexes.

1700 turnovers/hour for **1** and 1100/hour for **2**. The microstructure of the polymer is illustrated below. The polymer is regioregular, and the chain bears a methyl group on every third carbon. The ^{13}C NMR analysis established a totally atactic stereochemistry. Curiously, although *trans*-2-butene is polymerized with good activity, we were unable to observe polymer formation from *cis*-2-butene. Coates has reported formation of a partially isotactically enriched polymer using α-diimine Ni(II) catalysts constructed to possess C_2 symmetry.[21] In these cases only *trans*-2-butene yielded polymer.

In this article we report the homopolymerization of *cis*- and *trans*-2-butenes by Pd(II) diimine complexes and an in-depth mechanistic study that provides insight into the differences in behavior of these monomers toward both Ni(II) and Pd(II) diimine catalysts.

Results and Discussion

Polymerization of *trans*- and *cis*-2-Butenes. The catalysts employed for the copolymerization reactions were the cationic α-diimine palladium complex **3** and **4** (Scheme 2). The α-diimine ligands[22] and the palladium chloride complexes,[4] [(ArN=C(An)−(An)C=NAr)-Pd(Me)(Cl)], were synthesized following the procedures in the literature. The cationic complexes **3** and **4** were prepared in an analogous manner to the procedure published for the corresponding compound [(ArN=C(Me)−(Me)C=NAr)Pd(Me)(NCAr′)].[23]

The activity of α-diimine palladium complex **3** and **4** for the polymerization of 2-butenes was investigated. Both catalysts were found to be active for the polymerization of both *trans*- and *cis*-2-butene without the need for an activator or cocatalyst. Polymerizations were initiated by the addition of the palladium catalyst to a butene-saturated solution in a glass pressure reaction vessel (Fischer−Porter bottle) and stirring under monomer pressure. The polymerization results are summarized in Table 1.

The results show that with the same catalyst and under similar reaction conditions, the productivity (shown as turnover number, TON) of *cis*-2-butene polymerization is much lower than that for *trans*-2-butene. The reasons for this difference in reactivity are addressed

(15) Natta, G.; Dall'asta, G.; Mazzanti, G.; Pasquon, I.; Valvassori, A.; Zambelli, A. *J. Am. Chem. Soc.* **1961**, *83*, 3343.
(16) Natta, G. *Pure Appl. Chem.* **1962**, *4*, 363.
(17) Longo, P.; Grisi, F.; Guerra, G.; Cavallo, L. *Macromolecules* **2000**, *33*, 4647−4659.
(18) Ahn, C.-H.; Tahara, M.; Uozumi, T.; Jin, J.; Tsubaki, S.; Sano, T.; Soga, K. *Macromol. Rapid Commun.* **2000**, *21*, 385−389.
(19) It has been reported that Ti and V catalyst systems successfully catalyze the homopolymerization of internal olefins, but it is believed that the polymerization occurs because the internal olefins isomerize to form α-olefins first. This process is termed a monomer-isomerization polymerization. Addition of group VIII transition metal compounds such as NiX_2 (X = Br, Cl), which are known to be good isomerization catalysts, accelerates such polymerization reactions. (a) Endo, K.; Ueda, R.; Otsu, T. *J. Polym. Sci., Polym. Chem.* **1991**, *29*, 807−812. (b) Endo, K.; Ueda, R.; Otsu, T. *Macromolecules* **1991**, *24*, 6849−6852. (c) Endo, K.; Ueda, R.; Otsu, T. *Polym. J.* **1991**, *23*, 1173−1178. (d) Endo, K.; Ueda, R.; Otsu, T. *Makromol. Chem.* **1992**, *193*, 539−547. (e) Endo, K.; Ueda, R.; Otsu, T. *Makromol. Chem.* **1993**, *194*, 2623.
(20) Leatherman, M. D.; Brookhart, M. *Macromolecules* **2001**, *34*, 2748−2750.
(21) Cherian, A. E.; Lobkovsky, E. B.; Coates, G. W. *Chem. Commun.* **2003**, *20*, 2566−2567.
(22) van Koten, G.; Virieze, K. *Adv. Organomet. Chem.* **1982**, *21*, 151−239.
(23) Mecking, S.; Johnson, L. K.; Wang, L.; Brookhart, M. *J. Am. Chem. Soc.* **1998**, *120*, 888−899.

Scheme 2. Synthesis of α-Diimine Pd(II) Catalysts 3 and 4

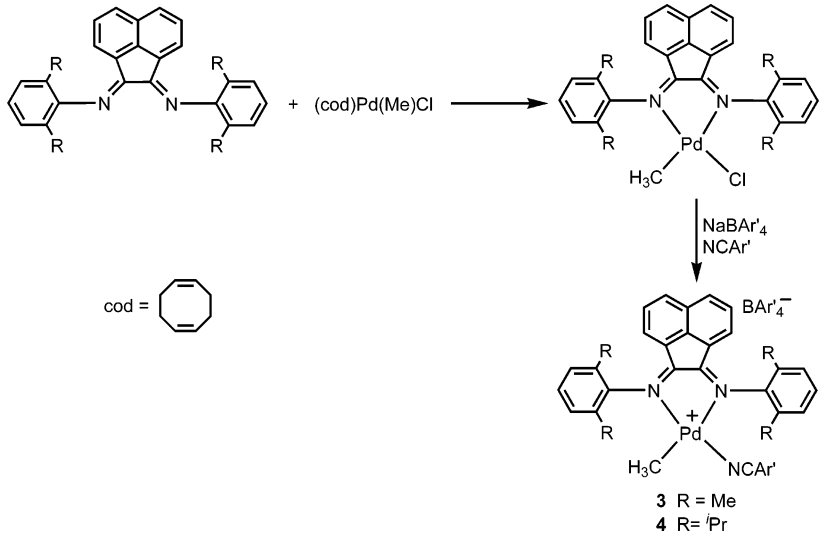

Table 1. *trans*- and *cis*-2-Butene Polymerization Data[a]

entry	catalyst	2-butene	pressure/ psi	TON[b]	M_n[c]	branches/ 1000C[c]
1	**3**	*trans*	14	1110	25 800	264
2	**3**	*cis*	13	180	2300	294
3	**4**	*trans*	14	390	24 800	264
4	**4**	*cis*	13	120	2200	281

[a] Reaction conditions: 10 μmol of catalyst, 15 mL of toluene, 25 °C, 3 h. [b] TON: turnover number. [c] Determined by ^{1}H NMR spectroscopic analysis of the polymer.

by mechanistic studies described below. At the same time, the molecular weight of poly(*cis*-2-butene) is ca. 11 times lower than that of poly(*trans*-2-butene). This is thought to be mainly due to the slow propagation rate of *cis*-2-butene as well as the relative chain transfer rates. For example, with catalyst **3**, each palladium center undergoes, on average, ca. two chain transfers during *trans*-2-butene polymerization (entry 1), while about four chain transfers occur on average during *cis*-2-butene polymerization (entry 2). This difference in relative chain transfer rates together with the difference in propagation rates account for the lower molecular weight of poly(*cis*-2-butene).

Increasing the steric bulk of the ortho aryl substituent from methyl to isopropyl results in a decrease in productivity, while the molecular weights of polymer produced remain basically the same.

Analysis by ^{1}H NMR spectroscopy indicates that the polymers contain slightly more than half (260−290) the number of branches per 1000 carbon atoms expected from standard 2-butene enchainment (500 branches/1000C). As shown in Figure 3, the ^{13}C NMR spectrum of the polymer is similar to that for the poly(*trans*-2-butene) produced by nickel catalysts[20] and shows distinct methyl (20.1 ppm), methylene (34.8 ppm), and methine (33.6 ppm) carbon resonances, which is consistent with a regioregular polymer microstructure carrying a methyl branch on every third carbon. The ca. 1:2:1 pattern of methyl resonance indicates an atactic microstructure with a 1:2:1 ratio of rr:mr:mm dyads. The minor resonances at 11.6 and 30.5 ppm belong to the methyl and methylene carbons, respectively, of the repeat units with ethyl branches, $-CH_2-CH(CH_2CH_3)-$.

Migratory Insertion of *trans*-2-Butene and *cis*-2-Butene: Barriers. The precursor employed for generation of 2-butene complexes is the cationic α-diimine palladium complex **5** (Scheme 3), which was synthesized using procedures in the literature.[4,24] Addition of ca. 4 equiv of *trans*-2-butene to a CD_2Cl_2 solution of **5** at −80 °C leads to clean formation of the η^2-olefin complex **6**. The displacement is fast and complete at this temperature. Key ^{1}H NMR resonances for the η^2-*trans*-2-butene complex **6** include δ 5.16 and 4.52 ppm for the bound olefinic protons and δ 0.51 ppm for the Pd−CH_3 methyl group. Complex **6** is stable when the temperature is below −30 °C, and no measurable migratory insertion was observed at this stage.

Migratory insertion of the *trans*-2-butene occurs at −30 °C and higher temperatures, yielding exclusively the η^2-olefin palladium alkyl complex **8**, which is assumed to be formed from the direct 2,3-insertion product **7** via a chain-straightening isomerization mechanism as proposed in Scheme 4. The chain-straightening process involves β-hydride elimination, olefin rotation, and reinsertion. Neither complex **7** nor other intermediates were observed under these conditions, presumably due to the fast rate of the isomerization and trapping processes. No identifiable ethyl-branched alkyl product was observed, which indicates that pathway A is favored over pathway B (Scheme 4) probably due to less favored trapping of the β-substituted primary alkyl species **10** relative to **9**.[25] Key ^{1}H NMR features of the insertion product **8** include δ 0.59 and 0.40 ppm resonances for

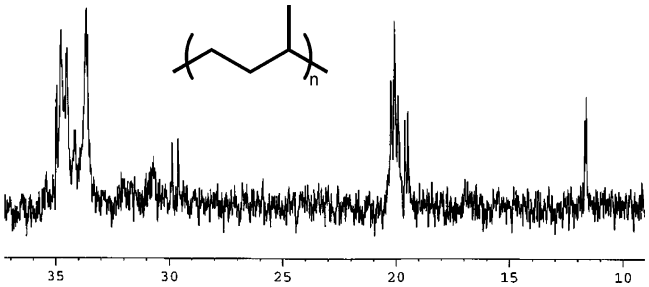

Figure 3. ^{13}C NMR spectrum of poly(*trans*-2-butene).

Scheme 3. Synthesis of α-Diimine Pd(II) Catalysts 3 and 4

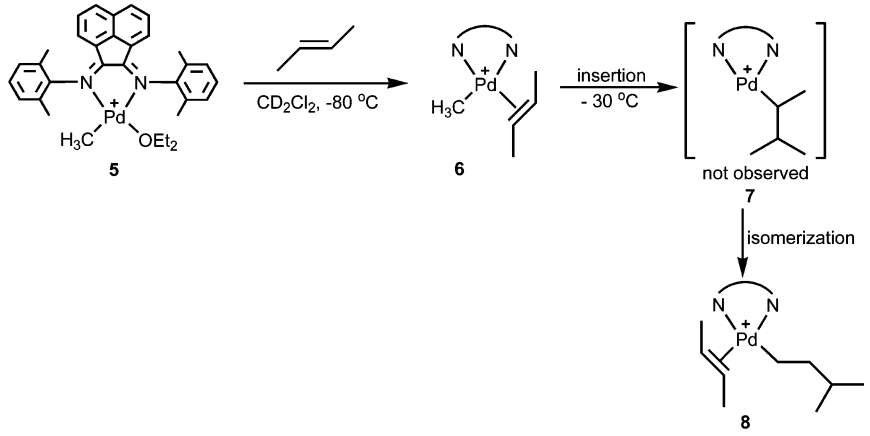

Scheme 4. Proposed Pd(II)-Catalyzed 2-Butene Polymerization Mechanism

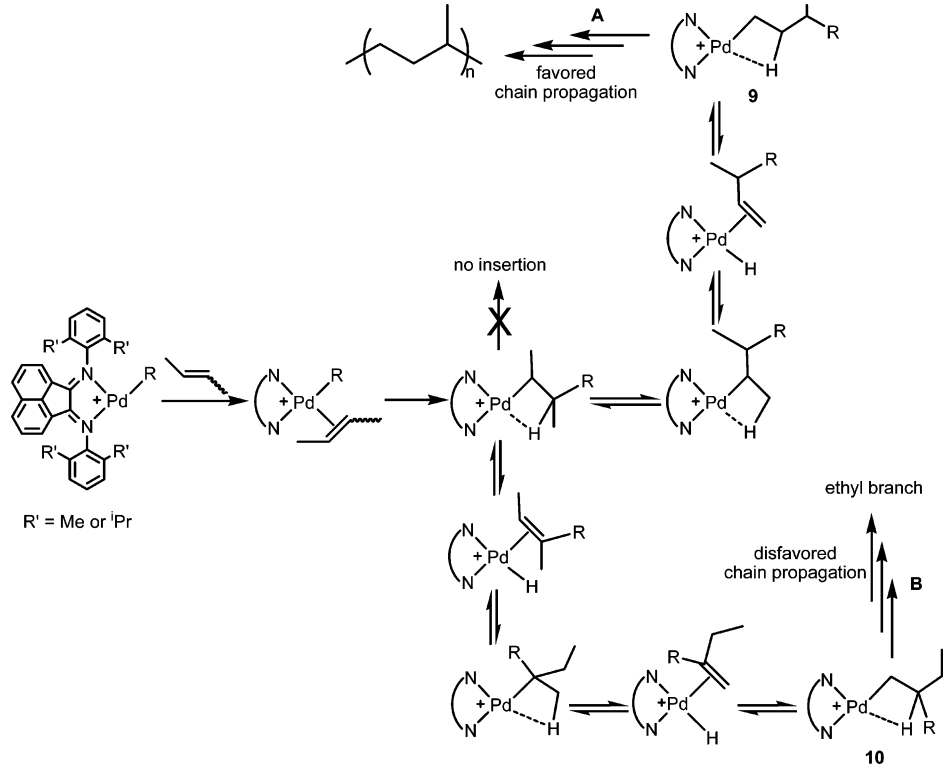

the diastereotopic methyl groups at the terminus of the alkyl chain, and δ 4.83 and 4.68 ppm vinylic signals of the bound *trans*-2-butene. At −30 °C, no significant amount of subsequent insertion product was observed.

The energy barrier ($\Delta G^{\ddagger}$) of *trans*-2-butene migratory insertion was determined to be 19.1 ± 0.1 kcal/mol at −20 °C by following the disappearance of the Pd−CH_3 signal (complex **6**) by ^{1}H NMR spectroscopy. The barrier is about 0.7 kcal/mol higher than that for ethylene migratory insertion to the Pd−Me bond in the analogous system ($\Delta G^{\ddagger}$ = 18.4 kcal/mol at −20 °C),[24] which means that the insertion rate of ethylene is ca. 4 times faster than that of *trans*-2-butene at this temperature.

The insertion chemistry of *cis*-2-butene was also investigated. Treatment of **5** with ca. 4 equiv of *cis*-2-butene in CD_2Cl_2 at −80 °C results in clean formation of the η^2-olefin complex **11** (Scheme 5). Similar to the case of *trans*-2-butene, the displacement is fast and complete at this temperature. Key ^{1}H NMR resonances for the η^2-*cis*-2-butene complex **11** include δ 5.12 ppm for the bound olefinic protons and δ 0.33 ppm for the Pd−CH_3 methyl group. Complex **11** is also stable when the temperature is below −30 °C, and no measurable migratory insertion was observed at this stage.

Similar migratory insertion behavior as seen in the *trans*-2-butene case was observed at −30 °C and higher temperatures, yielding exclusively the η^2-olefin palladium alkyl complex **12**, the product formed from the direct 2,3-insertion to yield **7** followed by isomerization via the mechanism proposed in Scheme 5. The 2,3-insertion product **7** is identical to the one for *trans*-2-butene insertion (Scheme 3) and was not observed. Again, no identifiable ethyl branched alkyl product was observed. Key ^{1}H NMR resonances of the insertion

(24) Tempel, D. J.; Johnson, L. K.; Huff, R. L.; White, P. S.; Brookhart, M. *J. Am. Chem. Soc.* **2000**, *122*, 6686−6700.
(25) Shultz, L. H.; Tempel, D. J.; Brookhart, M. *J. Am. Chem. Soc.* **2001**, *123*, 11539−11555.

Scheme 5. Migratory Insertion of *cis*-2-Butene into the Pd−Me Bond of Complex 5

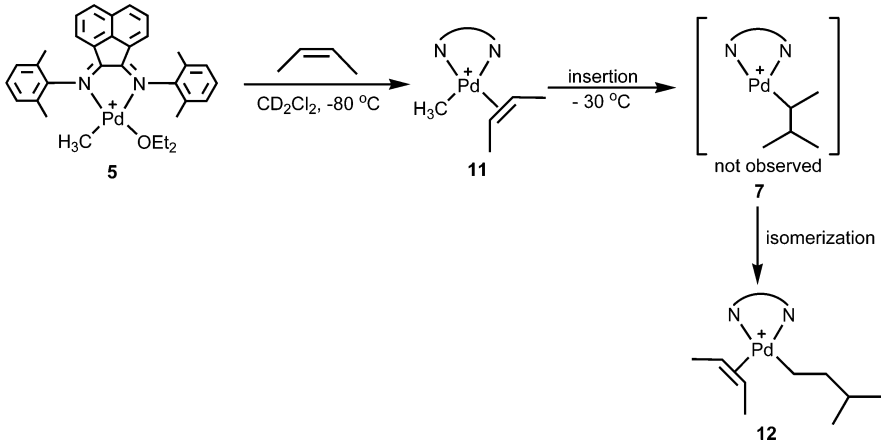

product **12** appear at δ 0.46 ppm for the two equivalent methyl groups at the end of the alkyl chain, δ 5.24 ppm for the olefinic protons of bound *trans*-2-butene, and δ 1.19 ppm for the methylene protons of Pd−CH_2. At −30 °C, no significant amount of subsequent insertion product was observed.

The energy barrier ($\Delta G^{\ddagger} = 19.3 \pm 0.1$ kcal/mol) of *cis*-2-butene migratory insertion was determined in a manner similar to that for *trans*-2-butene by ^{1}H NMR spectroscopy at −20 °C. The barrier is about 0.2 kcal/mol higher than that for *trans*-2-butene migratory insertion ($\Delta G^{\ddagger} = 19.1$ kcal/mol at −20 °C), which shows that the first insertion rate of *trans*-2-butene is only slightly faster (ca. 1.6-fold) than that of *cis*-2-butene at this temperature. This difference is less than that in the real polymerization reactions (Table 1, entries 1 and 2), where the *trans*-2-butene propagation rate is ca. 6 times faster than that for *cis*-2-butene under similar reaction conditions.

Rates of Subsequent Insertion Reactions. Subsequent insertions of *trans*- and *cis*-2-butenes into the growing polymer chain, which mimic the real chain propagation during the polymerization reactions, were investigated by following the decreasing signal for free *trans*- and *cis*-2-butenes in the solution in the presence of complex **8** or **12**.

The rate of the subsequent insertion of *trans*-2-butene (eq 1) was measured in CD_2Cl_2 at −10 °C, and the corresponding activation barrier is 19.6 ± 0.1 kcal/mol, which is ca. 0.5 kcal/mol higher than the barrier of first insertion ($\Delta G^{\ddagger} = 19.1$ kcal/mol at −10 °C). This follows the same trend as ethylene homopolymerization chemistry, where the barrier for subsequent insertion ($\Delta G^{\ddagger} = 18.6$ kcal/mol at −20 °C) is about 0.2 kcal/mol higher than that of the first insertion ($\Delta G^{\ddagger} = 18.4$ kcal/mol at −20 °C).[24]

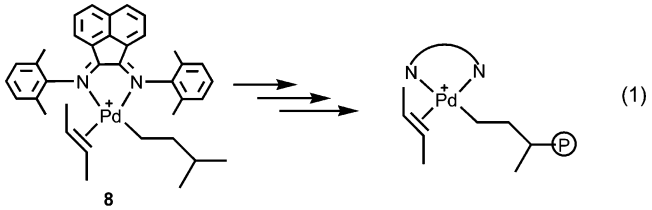

(1)

Similarly, the subsequent insertion (eq 2) rate for *cis*-2-butene was measured at −10 °C. The corresponding energy barrier is 20.2 ± 0.1 kcal/mol, which is ca. 0.9 kcal/mol higher than that for the first insertion of *cis*-2-butene ($\Delta G^{\ddagger} = 19.3$ kcal/mol at −10 °C). Compared with the insertion barrier for *trans*-2-butene, this activation barrier is 0.6 kcal/mol higher, which corresponds to a ca. 3-fold difference in insertion rates at this temperature.

Relative Binding Affinities. For bulky internal olefins such as *trans*- and *cis*-2-butenes, their binding affinities to the metal center could possibly affect the productivities of the transition metal catalyzed polymerization reactions, given the fact that there are often some stronger ligands such as acetonitrile and benzonitrile in the reaction mixture.

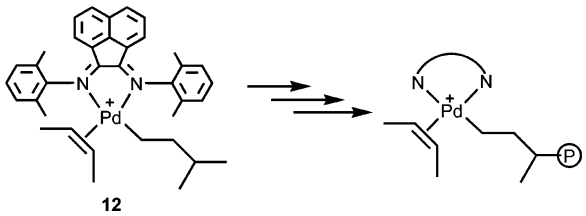

(2)

The relative binding affinities of *trans*- and *cis*-2-butenes were investigated using ^{1}H NMR spectroscopy. The equilibrium constants for the reactions depicted in eq 3 were determined by low-temperature ^{1}H NMR spectroscopy and are summarized in Table 2. The equilibrium constant could not be precisely measured in a single competition experiment because the resonances of *trans*- and *cis*-2-butenes overlap with each other. Trimethoxyvinylsilane was chosen as a comparison ligand because its spectrum is clearly separated from those of *trans*- and *cis*-2-butenes. The relative binding affinities of *trans*-2-butene versus trimethoxyvinylsilane and *cis*-2-butene versus trimethoxyvinyl-

Table 2. Equilibrium Constants for Eq 3

entry[a]	T (°C)	L	L′	K_{eq}	ΔG (kcal/mol)
1	−70	trimethoxyvinylsilane	*cis*−2-butene	3.4	−0.49
2	−70	trimethoxyvinylsilane	*trans*-2-butene	0.66	0.17
3	−70	*trans*-2-butene	*cis*−2-butene	5.1[b]	−0.66
4	−60	trimethoxyvinylsilane	*cis*−2-butene	3.0	−0.46
5	−60	trimethoxyvinylsilane	*trans*-2-butene	0.96	0.017
6	−60	*trans*-2-butene	*cis*−2-butene	3.1[b]	−0.48
7	−50	trimethoxyvinylsilane	*cis*−2-butene	2.9	−0.47
8	−50	trimethoxyvinylsilane	*trans*-2-butene	1.4	−0.15
9	−50	*trans*-2-butene	*cis*−2-butene	2.0[b]	−0.32

[a] Solvent: CD_2Cl_2. [b] Calculated.

silane were determined and used to calculate the relative binding affinities of *trans*-2-butene versus *cis*-2-butene as given by K_{eq} for the equation in eq 3, where L = *trans*-2-butene, L′ = *cis*-2-butene.

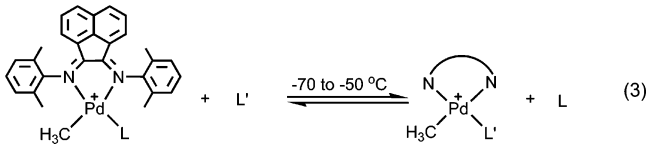

Results show that *cis*-2-butene binds slightly more strongly than *trans*-2-butene at low temperatures. At −70 °C, the equilibrium constant is ca. 5.1 (corresponding $\Delta G = -0.66$ kcal/mol), while it is 3.1 (corresponding $\Delta G = -0.48$ kcal/mol) at −60 °C and 2.0 (corresponding $\Delta G = -0.32$ kcal/mol) at −50 °C. A rough Van't Hoff analysis yields approximate enthalpy and entropy values for the equilibrium ($\Delta H = -4.1$ kcal/mol, $\Delta S = -17$ eu). From these data the equilibrium constant at 25 °C was calculated to be 0.2, which means the palladium center slightly favors *trans*-2-butene over *cis*-2-butene under polymerization reaction conditions.

Considering that the palladium methyl complexes **6** and **11** are not good models for the real polymerization system, dialkyl palladium complex **13** (Scheme 6) was employed for further investigation of the binding affinities of the 2-butenes. The palladium dichloride complexes [(ArN=C(An)−(An)C=NAr)Pd(Cl)$_2$] were synthesized following the procedure in the literature.[26] Complex **13** was synthesized in a manner analogous to the procedure published for the corresponding compound [(ArN=C(An)−(An)C=NAr)Pd(*n*-Pr)$_2$].[25]

Addition of 1 equiv of HBAr′(OEt$_2$)$_2$ to the solution of **13** in CD_2Cl_2 at −78 °C results in formation of 1 equiv of 2-methylpentane and two β-agostic complexes, **14a** and **14b**, in a ratio of ca. 3:1, as evidenced by two broad agostic hydrogen signals at −7.35 and −7.25 ppm. The downfield signals, which partially overlap the resonances of 2-methylpentane, are broadened due to rapid isomerization, and structures of the isomers present cannot be definitively assigned. However, treatment of these agostic species with either *trans*-2-butene or *cis*-2-butene results in clean formation of **8** or **12**, respectively (Scheme 7). These trapping experiments, which yield the most stable primary alkyl complexes, are consistent with our earlier reports of similar trapping experiments.[25]

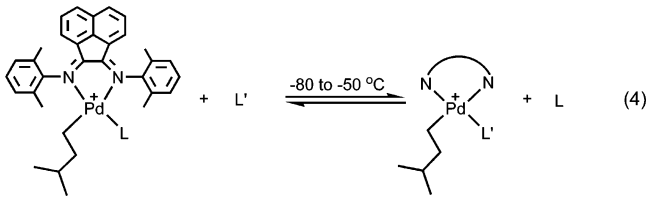

Clean generation of either **8** or **12** allows study of the relative binding affinities as generally illustrated by reactions in eq 4. The equilibrium constants of these reactions were measured by low-temperature ^{1}H NMR spectroscopy and are summarized in Table 3. Trimethoxyvinylsilane was again used as a comparison ligand for the same reason as above. The equilibrium constants of the *trans*-2-butene/trimethoxyvinylsilane pair and trimethoxyvinylsilane/*cis*-2-butene pair were used to calculate the relative binding affinities of *trans*-2-butene versus *cis*-2-butene as given by K_{eq} for the equation shown in eq 4, where L = *trans*-2-butene and L′ = *cis*-2-butene.

Results show that there is almost no difference between the binding strength of *trans*-2-butene and that of *cis*-2-butene. At −80 °C, the equilibrium constant is ca. 0.94 (corresponding $\Delta G = 0.02$ kcal/mol), while it is 1.0 (corresponding $\Delta G = 0.00$ kcal/mol) at −70 °C and 1.1 (corresponding $\Delta G = -0.04$ kcal/mol) at −60 °C. Earlier studies showed that in the polymerization of α-olefins using nitrile complexes analogous to **3** and **4** the catalyst resting state was an equilibrium mixture of the α-olefin complex and the nitrile complex.[27] In the case of the bulkier 2-butenes, this equilibrium clearly will be shifted more to the side of the nitrile complex. Thus, relative binding affinities of the two olefins, *cis*- and *trans*-2-butene, could play a significant role in their relative polymer propagation rates. However, the fact that the binding affinities of the two olefins are nearly

Scheme 6. Synthesis of Pd(II) Dialkyl Complex 13

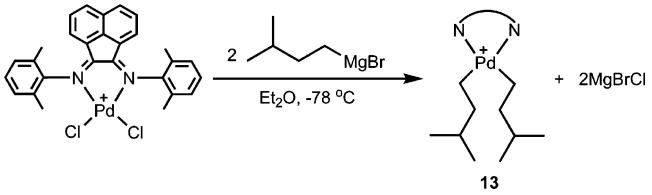

Scheme 7. Trapping of Agostic Cations 14a,b with 2-Butenes

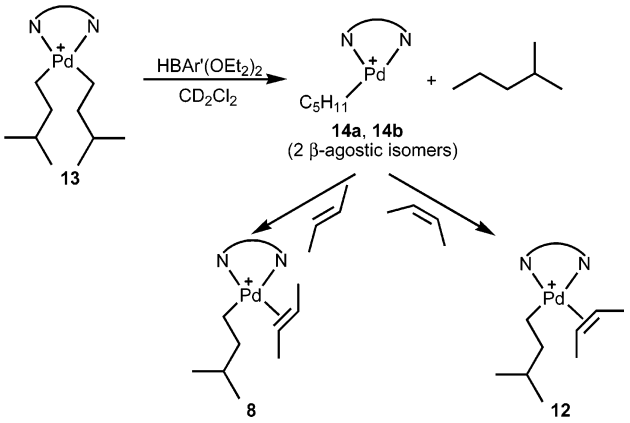

Table 3. Equilibrium Constants for Eq 4

entry[a]	T (°C)	L1	L2	K_{eq}	ΔG (kcal/mol)
1	−80	trimethoxyvinylsilane	*cis*-2-butene	1.6	−0.18
2	−80	trimethoxyvinylsilane	*trans*-2-butene	1.7	−0.20
3	−80	*trans*-2-butene	*cis*-2-butene	0.94[b]	0.02
4	−70	trimethoxyvinylsilane	*cis*-2-butene	2.0	−0.28
5	−70	trimethoxyvinylsilane	*trans*-2-butene	2.0	−0.28
6	−70	*trans*-2-butene	*cis*-2-butene	1.0[b]	0.00
7	−60	trimethoxyvinylsilane	*cis*-2-butene	2.3	−0.35
8	−60	trimethoxyvinylsilane	*trans*-2-butene	2.1	−0.31
9	−60	*trans*-2-butene	*cis*-2-butene	1.10[b]	−0.04

[a] Solvent: CD_2Cl_2. [b] Calculated.

(26) Shultz, L. H.; Brookhart, M. *Organometallics* **2001**, *20*, 3975−3982.

(27) Gottfried, A. C.; Brookhart, M. *Macromolecules* **2003**, *36*, 3085−3100.

identical suggests that the main factor in dictating the higher propagation rate of *trans*- versus *cis*-2-butene is the lower insertion barrier of the *trans*-2-butene relative to the *cis*-2-butene.

Summary

The α-diimine Pd(II) catalysts described here allow for the polymerization of both *trans*- and *cis*-2-butenes, although the productivities are much lower than those for α-diimine Ni(II)-catalyzed *trans*-2-butene polymerizations. The polymers exhibit atactic regioregular microstructure with a methyl branch on every third backbone carbon due to the chain-straightening mechanism. Both the productivity and the molecular weight of poly(*cis*-2-butene) are much lower than those of poly(*trans*-2-butene).

Mechanistic aspects of the polymerization reactions were investigated by low-temperature NMR spectroscopy. The isopentyl palladium complexes **14a** and **14b**, which most closely model the propagating species, exhibit nearly equal binding affinities for *cis*- and *trans*-2-butene. The barriers to migratory insertion of the *cis*- and *trans*-2-butene adducts **6** and **11** of the palladium methyl complex and the adducts **8** and **12** of the palladium isopentyl complex were measured. For the latter two complexes, which best model the propagating species, the insertion barrier for the *trans*-2-butene complex (19.6 kcal/mol) is ca. 0.6kcal/mol less than the barrier for migratory insertion of the *cis*-2-butene complex (20.2 kcal/mol). From these data we conclude that the primary factor in determining the lower propagation rate of the *cis*-2-butene relative to the *trans*-2-butene is the lower barrier of migratory insertion of the *trans* olefin.

In contrast to the Pd system, the nickel diimine systems show a much greater difference in activities: *trans*-2-butene is quite reactive and yields high polymer with a turnover frequency of ca. 1700/h at 25 °C using the complex analogous to **3**. In the case of the *cis* isomer no polymer (or oligomer) is observed. On the basis of earlier results for α-olefins[28] it is clear the catalyst resting state is Ni agostic species. Thus, the relative activities are determined by both the difference in binding affinities and insertion barriers. On the basis of the results for the Pd systems, it is likely that the major determining factor is the difference in insertion barriers.

Experimental Section

General Methods. All manipulations of air- and/or water-sensitive compounds were performed using standard high-vacuum or Schlenk techniques. Argon was purified by passage through columns of BASF R3-11 catalyst (Chemalog) and 4 Å molecular sieves. Solid organometallic compounds were transferred in argon-filled Vacuum Atmospheres or MBraun dryboxes and were stored in the drybox. ^{1}H and ^{13}C NMR spectra were recorded on Bruker Avance 300 or 500 MHz spectrometers. Chemical shifts are reported in ppm downfield of TMS and are referenced to residual ^{1}H NMR signals and to the ^{13}C NMR signals of the deuterated solvents, respectively.

Error analysis of $\Delta G^{\ddagger}$ was based on Binsch's derivation of $\sigma\Delta G^{\ddagger}$ and incorporated an estimate of 10% error in k and ±1 °C error in temperature.[29]

Materials. Diethyl ether, pentane, and methylene chloride were purified using procedures recently reported by Pangborn et al.[30] High-purity (99.0+ %) *trans*-2-butene and *cis*-2-butene were purchased from Aldrich Chemical Co. and used without further purification. The α-diimine ligands (ArN=C(An)−C(An)=NAr, An = acenaphthyl = 1,8-naphth-diyl)[22] and corresponding (α-diimine)palladium(II) chloride complexes[24] were prepared according to literature procedures. Palladium methyl ether adduct **3**,[4,24] (cod)Pd(Me)(Cl),[31] and $[H(OEt_2)_2]^+[BAr'_4]^-$ ($BAr'_4{}^-$ = $B(3,5\text{-}C_6H_3(CF_3)_2)_4{}^-$)[32] were prepared according to literature procedures. Dichloromethane-d_2 was dried over P_2O_5 or CaH_2, vacuum transferred, degassed by three freeze−pump−thaw cycles, and stored over activated 4 Å molecular sieves. Acenaphthenequinone, 2,6-dimethylaniline, and 2,6-diisopropylaniline were purchased from Aldrich Chemical Co. and used without further purification. $NaBAr'_4$ was purchased from Boulder Scientific and dried in vacuo over P_2O_5 for 3 days. (Cyclooctadiene)$PdCl_2$ was purchased from Strem Chemicals and used as received. 1-Bromo-3-methylbutane was purchased from Aldrich Chemical Co. and used without further purification. $BrMg(CH_2)_2(CH)(CH_3)_2$ was prepared using a standard literature procedure[33] and titrated with 2-butanol and 1,10-phenathroline.

Synthesis of Catalysts. Spectral Data for the BAr'_4 Counterion. The following ^{1}H and ^{13}C spectroscopic assignments of the BAr'_4 counterion in CD_2Cl_2 were invariant for different complexes and temperatures and are not reported in the spectroscopic data for each of the cationic complexes.

$B[3,5\text{-}C_6H_3(CF_3)_2]_4{}^-$ (BAr'_4). ^{1}H NMR (CD_2Cl_2): δ 7.74 (s, 8H, H_o), 7.57 (s, 4H, H_p). $^{13}C\{^1H\}$ NMR (CD_2Cl_2): δ 162.2 (q, J_{CB} = 37.4 Hz, C_{ipso}), 135.2 (C_o), 129.3 (q, J_{CF} = 31.3 Hz, C_m), 125.0 (q, J_{CF} = 272.5 Hz, CF_3), 117.9 (C_p).

Synthesis of $[(ArN{=}C(An){-}C(An){=}NAr)Pd(Me)(NCAr')]^+BAr'_4{}^-$ (Ar = 2,6-$Me_2C_6H_3$) (3). This complex was synthesized on the basis of literature procedures for the analogous complex with the methyl-substituted backbone.[23] A flame-dried Schlenk flask was charged with $NaBAr'_4$ (0.1624 g, 1.83 × 10^{-4} mol) and [(ArN=C(An)−C(An)=NAr)Pd(Me)(Cl)] (0.100 g, 1.83 × 10^{-4} mol) in a drybox under an argon atmosphere. The Schlenk flask was cooled to −78 °C, and CH_2Cl_2 (10 mL) was added via syringe. 3,5-Bis-trifluoromethylbenzonitrile (0.61 mL, ca. 20 equiv) was added, followed by another portion of CH_2Cl_2 (6 mL). The resulting bright maroon solution was allowed to warm to room temperature and stirred overnight. The reaction mixture was filtered, leaving behind a white precipitate of NaCl. The solvent was removed in vacuo, leaving a dark orange oil. Pentane (15 mL) was added to the oil, and the mixture was vigorously stirred for 1.5 h, during which time a yellow solid precipitated from the light orange solution. The solid was filtered and dried in vacuo for 3 h, yielding 0.276 g of yellow powder (94%). ^{1}H NMR (CD_2Cl_2, 300 MHz, 25 °C): δ 8.26 (s, 1H, Ar′) 8.22 (d, 1H, J = 6.3 Hz, An: H_p), 8.19 (d, 1H, J = 6.3 Hz, An′: H_p), 8.16 (s, 2H, Ar′), 7.55 (m, 2H, An: H_m, An′: H_m), 7.37 (m, 6H, H_{aryl}), 6.99 (d, 1H, J = 7.2 Hz, An:H_o), 6.63 (d, 1H, J = 7.2 Hz, An′:H_o), 2.42 and 2.31 (s, 6H each; $C_6H_3\mathit{Me}_2$ and $C'_6H_3\mathit{Me}_2$), 0.86 (s, 3H; PdMe). ^{13}C NMR (CD_2Cl_2, 125 MHz, 25 °C): δ 176.9, (N=C(H)), 169.9 (N=C'(H)), 146.6, 143.2, 142.3, 133.8, 133.5, 133.1, 131.7, 130.0, 129.9, 129.6, 129.1, 128.9, 128.4, 128.3, 128.2, 125.5, 125.4, 125.2, 123.9, 123.3, 121.7, 121.1, 119.7, 111.5) (An: CH and quaternary C and Ar: C_{ipso}, C_o, C_p, C_m and Ar′: C_o, C_p),

(28) Svejda, S. A.; Johnson, L. K.; Brookhart, M. *J. Am. Chem. Soc.* **1999**, *121*, 10634−10635.
(29) Binsch, G. *Dynamic Nuclear Magnetic Resonance Spectroscopy*; Jackman, L., Cotton, F. A., Eds.; Academic Press: New York, 1975; p 77.
(30) Pangborn, A. B.; Giardello, M. A.; Grubbs, R. H.; Rosen, R. K.; Timmers, F. J. *Organometallics* **1996**, *15*, 1518−1520.
(31) Rulke, R. E.; Ernsting, J. M.; Spek, A. L.; Elsevier, C. J.; van Leeuwen, P. W. N. M.; Vrieze, K. *Inorg. Chem.* **1993**, *32*, 5769−5778.
(32) Brookhart, M.; Grant, B.; Volpe, A. F., Jr. *Organometallics* **1992**, *11*, 3920−3922.
(33) *Handbook of Grignard Reagents*; Silverman, G. S., Ed.; Dekker: New York, 1996.

18.2 and 17.9 (Ar(CH_3)$_2$ and Ar($C'H_3$)$_2$), 7.39 (PdCH_3). Anal. Calcd for ($C_{70}H_{42}BF_{30}N_3Pd$): C, 52.15; H, 2.62; N 2.61. Found: C, 52.43; H, 2.64; N, 2.63.

Synthesis of [(ArN=C(An)−C(An)=NAr)Pd(Me)(NCAr′)]$^+$BAr′$_4^-$ (Ar = 2,6-^{i}Pr$_2$C$_6$H$_3$) (4). This compound was synthesized using a procedure identical to that described above for **3**. Reagents used: NaBAr′$_4$ (0.1624 g, 1.83 × 10^{-4} mol), [(ArN=C(An)-C(An)=NAr)Pd(Me)(Cl)] (0.100 g, 1.83 × 10^{-4} mol), 3,5-bis-trifluoromethylbenzonitrile (0.61 mL, ca. 20 equiv). Following isolation of the crude product as an orange oil, pentane (15 mL) was added and the mixture was cooled to −78 °C overnight, during which time an orange solid precipitated from the solution. The solid was filtered and dried in vacuo for 3 h, yielding 0.186 g of orange powder (71%). ^{1}H NMR (CD_2Cl_2, 300 MHz, 25 °C): δ 8.26 (s, 1H, Ar′), 8.19 (d, 1H, J = 5.1 Hz, An: H$_p$), 8.17 (d, 1H, J = 3.0 Hz, An′: H$_p$), 8.16 (s, 2H, Ar′), 7.60 (m, 2H, An: H$_m$, An′: H$_m$), 7.49 (m, 6H, H$_{aryl}$), 6.98 (d, 1H, J = 7.2 Hz, An:H$_o$), 6.59 (d, 1H, J = 7.5 Hz, An′:H$_o$), 3.35 and 3.24 (m, 2H each; C_6H_3CH and C'_6H_3CH), 1,41 (d, 12H, $C_6H_3CH(Me)_2$), 1.09 and 1.01 (d, 6H each; $C'_6H_3CH(Me)_2$), 0.98 (s, 3H; PdMe). ^{13}C NMR (CD_2Cl_2, 125 MHz, 25 °C): δ 177.0 (N=C(H)), 170.2 (N=C'(H)), 146.5, 141.1, 140.2, 139.6, 139.0, 133.9, 133.2, 131.9, 130.0, 129.7, 129.2, 128.8, 128.2, 126.9, 126.0, 125.9, 125.5, 125.2, 125.0, 123.9, 123.2, 121.7, 121.1, 119.6, 115.2, 111.3) (An: CH and quaternary C and Ar: C$_{ipso}$, C$_o$, C$_p$, C$_m$ and Ar′: C$_o$, C$_p$), 29.8 and 29.6 (Ar(CH)(CH_3)$_2$ and Ar($C'H$)(CH_3)$_2$), 24.1, 23.9, 23.5, and 23.2 (Ar(CH)(CH_3)$_2$ and Ar(CH)($C'H_3$)$_2$ and Ar(CH)($C''H_3$)$_2$ and Ar(CH)($C'''H_3$)$_2$), 9.27 (PdCH_3). Anal. Calcd for ($C_{78}H_{58}BF_{30}N_3Pd$): C, 54.32; H, 3.39; N 2.44. Found: C, 54.05; H, 3.31; N, 2.57.

Synthesis of Dialkyl Complex. ((2,6-(CH$_3$)$_2$C$_6$H$_3$)N=C(An)−(An)C=N(2,6-(CH$_3$)$_2$C$_6$H$_3$))Pd(CH$_2$CH$_2$CH(Me)$_2$)$_2$ (13). A flame-dried Schlenk flask was charged with ((2,6-(CH$_3$)$_2$C$_6$H$_3$)-N=C(An)−(An)-C=N(2,6-(CH$_3$)$_2$C$_6$H$_3$))PdCl$_2$ (0.491 g, 0.87 mmol) in an argon-filled drybox. The flask was placed under argon and cooled to −78 °C (dry ice/2-propanol), and Et$_2$O (20 mL) was added via syringe. BrMg(CH$_2$CH$_2$CH(Me)$_2$) was added as a solution in Et$_2$O (0.3 M, 6 mL, 1.8 mmol), and the mixture was stirred at −78 °C for 2 h. MeOH (0.1 mL) was added to quench any excess Grignard reagent, and the dark mixture was flash-filtered through Florisil into a clean, flame-dried Schlenk at 0 °C. The Florisil was washed with Et$_2$O (10 mL) and pentane (10 mL), and the filtrate was reduced in vacuo to give a red-brown solid, which was dried under reduced pressure for 1 h at room temperature and stored at −30 °C in the drybox freezer. Yield: 0.330 g (60%). ^{1}H NMR (CD_2Cl_2, 500 MHz, −80 °C): δ 8.03 (d, 2H, J = 8.0 Hz, An: H$_p$), 7.42 (m, 2H, An: H$_m$, An′: H$_m$), 7.22 (m, 6H, H$_{aryl}$), 6.71 (d, 2H, J = 7.0 Hz, An:H$_o$), 2.27 (s, 12H $C_6H_3Me_2$), 1.09 (m, 4H, Pd(CH$_2$CH_2CHMe$_2$)$_2$), 1.02 (m, 2H, Pd(CH$_2$CH$_2$CHMe$_2$)$_2$), 0.87 (m, 4H, Pd(CH_2CH$_2$CHMe$_2$)$_2$), 0.58 (d, 12H, J = 6.5, Pd(CH$_2$CH$_2$CHMe_2)$_2$),. ^{13}C NMR (CD_2Cl_2, 125 MHz, −80 °C): δ 167.0, 145.7, 143.0, 130.1, 129.3, 128.7, 128.6, 128.2, 126.1, 123.2, 40.9 (PdCH$_2$CH$_2$$C$H(CH$_3$)$_2$), 32.5 (PdCH$_2$$CH_2$CH-(CH$_3$)$_2$), 22.5 (Pd$CH_2CH_2$CH(CH$_3$)$_2$), 18.1 (Ar$CH_3$), 16.9 (PdCH$_2CH_2$CH($CH_3$)$_2$). This compound was not sufficiently stable for elemental analysis.

General Procedure for Polymerization Reactions of *trans*- and *cis*-2-Butenes. An oven-dried Fischer−Porter bottle rated to 100 psi was equipped with a magnetic stir bar, attached to the pressure head unit, and repeatedly evacuated and backfilled with argon three times. Toluene (10 mL) was added via syringe and *trans*- or *cis*-2-butene pressure was added and released twice. The pressure was vented and a solution of the appropriate Pd(II) catalyst (0.010 mmol) in toluene (5 mL) was added quickly via cannula, and the reactor was sealed and brought to the appropriate monomer pressure. The reactor was stirred for the stated amount of time, then the excess pressure was vented, and the polymerization quenched with acetone (5 mL) and 6 M HCl (5 mL). The reaction solution was added dropwise to acidified methanol (150 mL), and the polymer was allowed to precipitate. The polymer was separated as a viscous oil and washed twice with methanol, then dried in a vacuum oven overnight at 50 °C.

In Situ Generation and NMR Observation of η^2-Olefin Pd(II) Complexes. In a drybox under an argon atmosphere, an NMR tube was charged with ca. 0.01 mmol of [(ArN=C(An)−C(An)=NAr)Pd(Me)(OEt$_2$)]BAr′$_4$. The tube was capped with a rubber septum and removed from the drybox. After securing the septum with Teflon tape and Parafilm, the tube was cooled to −78 °C. CD_2Cl_2 was added to the NMR tube via syringe (600 μL), and the septum was rewrapped with Parafilm. The tube was shaken and warmed slightly to facilitate dissolution of the complex. After acquiring a spectrum at −80 °C, olefin was added via syringe to the solution cooled to −78 °C, and the NMR tube was briefly shaken to completely dissolve the additive. The tube was then transferred to the precooled NMR probe for acquisition of spectra. The concentrations of the active species and free olefin were calculated using the BAr′$_4$ or *para*-acenaphthyl peaks as an internal standard.

[(ArN=C(An)−(An)C=NAr)Pd(CH$_3$)(η^2-*trans*-CH$_3$−CH=CH−CH$_3$)]$^+$[BAr′$_4$]$^-$ (Ar = 2,6-C$_6$H$_3$(CH$_3$)$_2$), 6. ^{1}H NMR (CD_2Cl_2, 500 MHz, −80 °C): δ 8.12 (d, 1H, J = 8.0 Hz, An: H$_p$), 8.09 (d, 1H, J = 8.5 Hz, An′: H$_p$), 7.47 (m, 2H, An: H$_m$, An′: H$_m$), 7.31 (m, 6H, H$_{aryl}$), 6.55 (d, 1H, J = 7.0 Hz, An: H$_o$), 6.46 (d, 1H, J = 7.0 Hz, An′: H$_o$), 5.16 and 4.52 (m, 1H each; Pd(η^2-*trans*-CH$_3$−CH=CH−CH$_3$)), 2.37, 2.20, 2.08, 1.98 (s, 3H each; Ar−CH_3), 1.76 and 1.64 (d, 3H each, J = 6.0; Pd(η^2-*trans*-CH_3−CH=CH−CH_3)), 0.51 (s, 3H; Pd(CH_3)).

[(ArN=C(An)−(An)C=NAr)Pd(CH$_3$)(η^2-*cis*-CH$_3$−CH=CH−CH$_3$)]$^+$[BAr′$_4$]$^-$ (Ar = 2,6-C$_6$H$_3$(CH$_3$)$_2$), 11. ^{1}H NMR (CD_2Cl_2, 500 MHz, −80 °C): δ 8.12 (d, 1H, J = 8.0 Hz, An: H$_p$), 8.09 (d, 1H, J = 8.0 Hz, An′: H$_p$), 7.47 (m, 2H, An: H$_m$, An′: H$_m$), 7.31 (m, 6H, H$_{aryl}$), 6.57 (d, 1H, J = 7.5 Hz, An: H$_o$), 6.51 (d, 1H, J = 7.5 Hz, An′: H$_o$), 5.12 (br m, 2H; Pd(η^2-*cis*-CH$_3$−CH=CH−CH$_3$)), 2.18, 2.16 (s, 6H each; Ar−CH_3), 1.68 (br d, 6H; Pd(η^2-*trans*-CH_3−CH=CH−CH_3)), 0.33 (s, 3H; Pd(CH_3)).

Determination of Rates of *trans*- and *cis*-2-Butene Migratory Insertion by NMR Spectroscopy. In a drybox under an argon atmosphere, an NMR tube was charged with ca. 0.01 mmol of [(ArN=C(An)−C(An)=NAr) Pd(Me)(OEt$_2$)]-BAr′$_4$. The tube was capped with a rubber septum and removed from the drybox. After securing the septum with Teflon tape and Parafilm, the tube was cooled to −78 °C. CD_2Cl_2 was added to the NMR tube via syringe (600 μL), and the septum was rewrapped with Parafilm. The tube was shaken and warmed slightly to facilitate dissolution of the complex. Then *trans*- or *cis*-2-butene was added via syringe to the solution cooled to −78 °C, and the NMR tube was briefly shaken to completely dissolve the additive. The tube was then transferred to the precooled NMR probe for acquisition of spectra. After acquiring a spectrum at −80 °C, the probe was warmed to proper temperature for the migratory insertion studies. The concentrations of the active species and free olefin were calculated using the BAr′$_4$ or *para*-acenaphthyl peaks as an internal standard. Rates of migratory insertion were determined by monitoring the loss of the PdCH_3 resonance. The natural logarithm of the starting alkyl olefin complex resonance was plotted versus time (first-order treatment) to obtain kinetic plots. NMR probe temperatures were calibrated using an Omega type T thermocouple immersed in anhydrous methanol in a 5 mm NMMR tube.

[(ArN=C(An)−(An)C=NAr)Pd(CH$_2$CH$_2$CH(CH$_3$)$_2$)(η^2-*trans*-CH$_3$−CH=CH−CH$_3$)]$^+$[BAr′$_4$]$^-$ (Ar = 2,6-C$_6$H$_3$(CH$_3$)$_2$), 8. ^{1}H NMR (CD_2Cl_2, 500 MHz, −20 °C): δ 8.16 (d, 1H, J = 8.0 Hz, An: H$_p$), 8.12 (d, 1H, J = 8.5 Hz, An′: H$_p$), 7.50 (m, 2H, An: H$_m$, An′: H$_m$), 7.35 (m, 6H, H$_{aryl}$), 6.57 (d, 1H, J = 7.5 Hz, An: H$_o$), 6.51 (d, 1H, J = 7.5 Hz, An′: H$_o$), 4.83 and 4.68 (m, 1H each; Pd(η^2-*trans*-CH$_3$−CH=CH−CH$_3$)), 2.35, 2.23,

2.21, 2.06 (s, 3H each; Ar−CH_3), 1.88 and 1.71 (d, 3H each, J = 6.0; Pd(η^2-*trans*-CH_3−CH=CH−CH_3)), 1.26 (br m, 3H; PdCH_2CH$_2$CH(CH$_3$)$_2$ and PdCH$_2$CH$_2$CH(CH$_3$)$_2$), 0.81 (m, 2H; PdCH$_2$CH_2CH(CH$_3$)$_2$), 0.59 and 0.40 (d, 3H each, J = 6.0; PdCH$_2$CH$_2$CH(CH_3)$_2$).

[(ArN=C(An)−(An)C=NAr)Pd(CH$_2$CH$_2$CH(CH$_3$)$_2$)(η^2-*cis*-CH$_3$−CH=CH−CH$_3$)]$^+$[BAr′$_4$]$^-$ (Ar = 2,6-C$_6$H$_3$(CH$_3$)$_2$), 12. ^{1}H NMR (CD$_2$Cl$_2$, 500 MHz, −20 °C): δ 8.17 (d, 1H, J = 8.5 Hz, An: H$_p$), 8.13 (d, 1H, J = 8.0 Hz, An′: H$_p$), 7.51 (m, 2H, An: H$_m$, An′: H$_m$), 7.35 (m, 6H, H$_{aryl}$), 6.62 (d, 1H, J = 7.0 Hz, An: H$_o$), 6.59 (d, 1H, J = 7.0 Hz, An′: H$_o$), 5.24 (m, 2H; Pd(η^2-*cis*-CH$_3$−CH=CH−CH$_3$)), 2.24, 2.23 (s, 6H each; Ar−CH_3), 1.72 (d, 6H each, J = 5.0; Pd(η^2-*cis*-CH_3−CH=CH−CH_3)), 1.19 (br m, 3H; PdCH_2CH$_2$CH(CH$_3$)$_2$ and PdCH$_2$-CH$_2$CH(CH$_3$)$_2$), 0.79 (m, 2H; PdCH$_2$CH_2CH(CH$_3$)$_2$), 0.46 (d, 6H, J = 6.5; PdCH$_2$CH$_2$CH(CH_3)$_2$).

Determination of Subsequent Insertion Rates by NMR Spectroscopy. In a drybox under an argon atmosphere, an NMR tube was charged with ca. 0.01 mmol of [(ArN=C(An)−C(An)=NAr)Pd(Me)(OEt$_2$)]BAr′$_4$. The tube was capped with a rubber septum and removed from the drybox. After securing the septum with Teflon tape and Parafilm, the tube was cooled to −78 °C. CD$_2$Cl$_2$ was added to the NMR tube via syringe (600 μL), and the septum was rewrapped with Parafilm. The tube was shaken and warmed slightly to facilitate dissolution of the complex. Then *trans*- or *cis*-2-butene was added via syringe to the solution at −78 °C, and the NMR tube was briefly shaken to completely dissolve the additive. The tube was then transferred to the precooled NMR probe for acquisition of spectra. The concentrations of the active species and free olefin were calculated using the BAr′$_4$ or *para*-acenaphthyl peaks as an internal standard. After the first insertion was complete, the probe was warmed to −10 °C and the zero-order disappearance of the free 2-butene integral was monitored.

In Situ Formation and NMR Observation of the β-Agostic Isopentyl Complexes. In a drybox under an argon atmosphere, an NMR tube was charged with ca. 0.01 mmol of [(ArN=C(An)−C(An)=NAr)Pd(CH$_2$CH$_2$CH(CH$_3$)$_2$)] (Ar = 2,6-C$_6$H$_3$(CH$_3$)$_2$) and 0.01 mmol of HBAr′(OEt$_2$)$_2$. The tube was capped with a rubber septum and removed from the drybox. After securing the septum with Teflon tape and Parafilm, the tube was cooled to −78 °C. CD$_2$Cl$_2$ was added to the NMR tube via syringe (600 μL), and the septum was rewrapped with Parafilm. The tube was shaken briefly to facilitate dissolution of the complex. The tube was then transferred to the precooled (−80 °C) NMR probe for acquisition of spectra.

[(ArN=C(An)−(An)C=NAr)Pd(CH$_2$(CH-μ-H)CH(CH$_3$)$_2$]$^+$-[BAr′$_4$]$^-$ (Ar = 2,6-C$_6$H$_3$(CH$_3$)$_2$), 14a,b. ^{1}H NMR (CD$_2$Cl$_2$, 500 MHz, −80 °C): δ 8.12 (d, 1H, J = 8.5 Hz, An: H$_p$), 8.09 (d, 1H, J = 8.5 Hz, An′: H$_p$), 7.49 (m, 2H, An: H$_m$, An′: H$_m$), 7.26 (m, 6H, H$_{aryl}$), 6.76 (d, 1H, J = 6.5 Hz, An: H$_o$), 6.63 (apparent t, 1H, J = 6.5 Hz, An′: H$_o$), 2.18 (br m, 6H; C$_6$H$_3$*Me*$_2$), 2.10 (m, 6H; C′$_6$H$_3$*Me*$_2$), 1.45, 0.88, and 0.45 (all br) for protons on the Pd alkyl chain, −7.25 and −7.35 (both br) for agostic protons. All Pd-alkyl resonances broadened due to exchange at this temperature. Isopentane is also present in the sample (δ 0.75 for methyl protons, 1.33 for the methine proton, methylene signals overlap with those of diethyl ether).

Relative Binding Affinity Studies. In a drybox under an argon atmosphere, an NMR tube was charged with ca. 0.01 mmol of [(ArN=C(An)−C(An)=NAr)Pd(Me)(OEt$_2$)]BAr′$_4$. The tube was capped with a rubber septum and removed from the drybox. After securing the septum with Teflon tape and Parafilm, the tube was cooled to −78 °C. CD$_2$Cl$_2$ was added to the NMR tube via syringe (600 μL), and the septum was rewrapped with Parafilm. The tube was shaken and warmed slightly to facilitate dissolution of the complex. Then appropriate amounts of *trans*- or *cis*-2-butene and trimethoxyvinylsilane were added via syringe to the solution at −78 °C, and again the NMR tube was briefly shaken to completely dissolve the additives. The tube was then transferred to the precooled (−80 °C) NMR probe for acquisition of spectra. The concentrations of the two complexes and the free olefins were calculated using the BAr′$_4$ or *para*-acenaphthyl peaks as an internal standard.

Acknowledgment. We thank DuPont and the National Science Foundation (CHE-0107810) for financial support of this work.

Supporting Information Available: Graphs for the determination of rates of migratory insertion. This material is available free of charge via the Internet at http://pubs.acs.org.

OM040077M